Preparation and Tribological Properties of a Multilayer Graphene-Reinforced TiO₂ Composite Nanolubricant Additive

Yu-kun Wei, Le-yang Dai,* Hai-chang Zhong, Hai-feng Liao, and Xian-bin Hou

ACCESS | Metrics & More | Article Recommendations

ABSTRACT: The unique structure and physical properties of graphene and anatase TiO₂ make them suitable for use as additives for engine lubricants. This study describes the use of dielectric barrier discharge plasma-assisted ball milling to synthesize a multilayer graphene-reinforced TiO₂ composite nanolubricant additive (MGTC). A variety of physical and chemical tests were performed to characterize the resulting experimental materials, including X-ray diffraction (XRD), Fourier transform infrared (FT-IR), Raman, X-ray photoelectron spectroscopy (XPS), and scanning electron microscopy (SEM). Four-ball friction and wear testing machines were used to study the tribological properties and extreme pressure anti-wear properties of a base oil containing 0.1, 0.5, 1.0, and 1.5 wt % of the modified TiO₂. Raman spectroscopy, XPS, SEM, and energy-dispersive spectrometry (EDS) analyses were used to examine and analyze the microstructure of the friction pairs. As a result of the plasma-assisted ball milling process, expanded graphite was successfully separated into multilayer graphene nanosheets, and spherical TiO₂ was successfully bonded to the nanosheets of the multilayer graphene. The 1.0 wt % composite oil was found to provide good friction reduction and wear resistance. It had a film thickness of 27.5 nm, which was 167% thicker than base oil. Due to its excellent dispersion stability, the MGTC nanocomposite exhibited excellent lubrication performance, which was attributed to the formation of carbon protective films, titanium dioxide deposition films, transfer films, and the occurrence of nano ball effects on the surface of friction pairs.
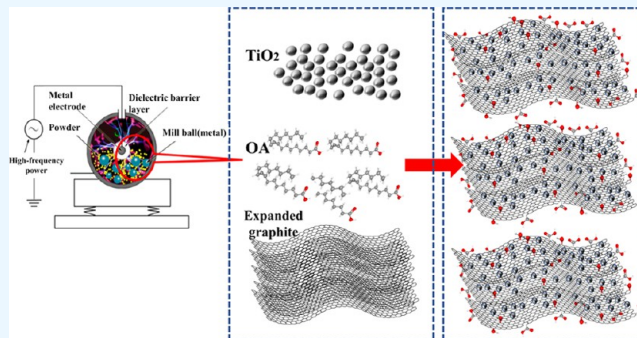
1. INTRODUCTION

The output power loss in marine diesel engines due to friction loss can reach 20%. On an annual basis, about 4−16% of the total fuel consumption of an engine is utilized to overcome frictional losses, which equates to 180 billion liters of diesel fuel.[1] Reducing friction loss is an effective means for improving an engine's dynamic performance.[2] The Stribeck curve can be divided into three different areas of lubrication: boundary lubrication, mixed lubrication, and elastohydrodynamic lubrication. Diesel engines have boundaries or mixed lubrication states at top dead center (TDC) and bottom dead center (BDC) and hydrodynamic lubrication states during the middle stroke position. The lubrication film is susceptible to thinning and break down when lubricating oil is applied to a micro-convex surface, such as in the process of boundary lubrication. This accounts for 40−50% of the total friction loss and has the highest coefficient of friction.[3] Therefore, improving the tribological characteristics of piston ring components is important for both improving engine performance and reducing emissions.

To improve the wear resistance of the engine piston ring, a chromium-coated cylinder liner is generally used. However, chromium-based coatings have the disadvantage that they are prone to wear and friction when operating in a nonlubricated state.[2] To improve the performance, reliability, and service life of internal combustion engines, extreme pressure lubricants are used to separate the contact surfaces.[4] The small size of added nanoparticles allows them to penetrate the friction area and fill in the wear marks, which prevents direct contact between the surfaces of the friction pair.[5] Precipitation is facilitated on friction surfaces with higher surface energies, and protective films form on worn surfaces. Base lubricants contain a variety of nanoadditives, including metals, metal oxides, nonmetal oxides, sulfides, and carbon compounds.[6] In recent years, nano TiO₂ has been widely used in engine lubricating oils due to its low cost, nontoxicity, excellent lubrication performance, and engineering applications. Among various tested lubricating oils, Wu et al. found that a base oil containing TiO₂ had the lowest
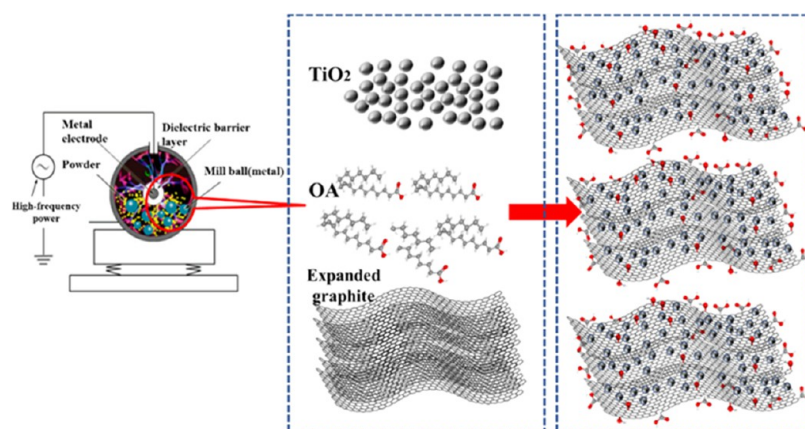
Figure 1. Schematic diagram of preparation of MGTC composite powder.

coefficient of friction because its viscosity was the highest.[7] According to Ali et al., nano TiO$_2$ and its rolling friction effect result in a 50% decrease in the friction coefficient of a piston ring assembly when used as lubricant additives.[8] Binu et al. found that TiO$_2$ nanoparticles could also act like ball bearings between friction pairs, and nanoparticles could form a protective layer on friction pairs by depositing onto their surfaces, thereby directly reducing friction and wear.[9]

Due to its two-dimensional lattice structure, graphene is an ideal additive for lubricants because of its exceptional mechanical strength, thermal stability, and low shear strength. Yin et al. found that graphene reduced friction and protected wear in wet and dry test environments by applying it to several typical friction pairs, such as bare steel, diamond-like, and ceramic materials.[10] Moreover, Restuccia et al. also demonstrated that the activity of graphene's unsaturated bonds can greatly reduce the friction pair surface's wear, so under both dry and wet conditions, it can be effectively used with steel—steel sliding contact surfaces.[11] These properties make graphene an excellent material for reducing friction and wear in diesel engines, such as piston rings and cylinder liners. According to Guo et al., multilayer graphene can withstand the load imposed by steel balls, avoiding direct contact with metal surfaces, reducing friction, and improving the anti-wear performance of base oils.[12] Eswaraiah et al. prepared ultrathin graphene using focused solar radiation. These authors confirmed that graphene's nano-bearing mechanism and its mechanical strength were the main properties responsible for its enhanced strength.[13] La et al. found that adding a modified graphene nanosheet additive to a lubricating oil (about 0.05%) increased the wear resistance of steel by more than 35%.[14] There is potential for using stripped graphene nanosheets for use as lubricating oil additives. These could be mass-produced at a low cost, which would enable practical application of graphene in the field of mechanical processing.

Adding two or more nanopowders to the base lubricant can produce an enhanced synergetic lubrication effect. Zhao et al. discussed the in situ synthesis of TiO$_2$/F-RGO nanocomposites and the use of nanocomposites as lubricant additives. TiO$_2$ nanoparticles and F-RGO nanosheets in nanocomposites have a synergistic lubrication effect and have demonstrated a low friction coefficient and excellent wear resistance.[15] Du et al. demonstrated that the excellent lubrication performance of GO-TiO$_2$ nanocomposites was due to its excellent dispersion stability and the formation of an adsorption film, a carbon protective film, and transfer film,

which resulted in good friction reduction and wear resistance.[16] Nano TiO$_2$ and graphene can be synergistically combined, resulting in a significant reduction in friction in comparison to pure nano TiO$_2$. The surface modification of nanopowders is affected by various factors such as synthetic conditions, and selecting suitable surface modifiers for high surface energy nanoparticles is challenging. Inorganic nanoparticles have a large surface area and high surface energy, which causes them to agglomerate in liquid media, which can increase wear on frictional surfaces. Our efforts have been directed toward developing DBDP-assisted ball milling, which is capable of simultaneously refining powders and modifying their surfaces to prepare high-quality nanocomposite powders in batches with high efficiency. By mechanical peeling, high-quality graphene can be prepared by dielectric barrier discharge plasma-assisted ball milling (DBDP). A multilayer graphene sheet that has been mechanically peeled exhibits superior lubrication and zero wear due to its perfect graphite structure and hydrophobic surface.[17] The more peeling there is, the more orderly the additives are under friction, so better lubrication can be achieved.[18] When the DBDP thermal explosion effect and pulsed electron bombardment effect are coupled, plasma-assisted ball milling can greatly shorten the powder nanometer preparation process.[19] Additionally, some polymers are more prone to bond breakage and polymerization under DBDP. Plasma-assisted ball milling also enables in situ surface modification of nanopowders by introducing active groups and coated polymers to the surface.[20] Therefore, plasma-assisted ball milling is a convenient method to prepare surface modification lubricant additives.

A simple and efficient method for preparing chemically functionalized graphene-based composite nanolubricating additives is presented in this paper. Using the plasma-assisted ball milling method to graft the oleophilic group onto the inorganic powder surface of expanded graphite and titanium dioxide, a graphene-supported titanium dioxide nanocomposites lubricant additive (MGTC) was prepared. Tests were conducted using 500 N as the base oil to examine the dispersibility and tribological properties of graphene-loaded titanium dioxide nanocomposites as lubricating additives. It was found that many organic molecules can be grafted onto graphene quickly and modified by plasma-assisted ball milling, resulting in improved graphene dispersion and wear resistance under extreme pressure.
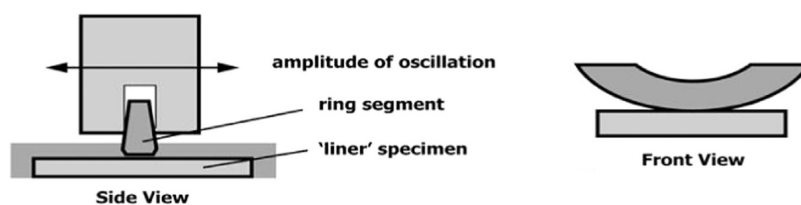
Figure 2. Piston ring and cylinder liner sample schematic drawing of the test.
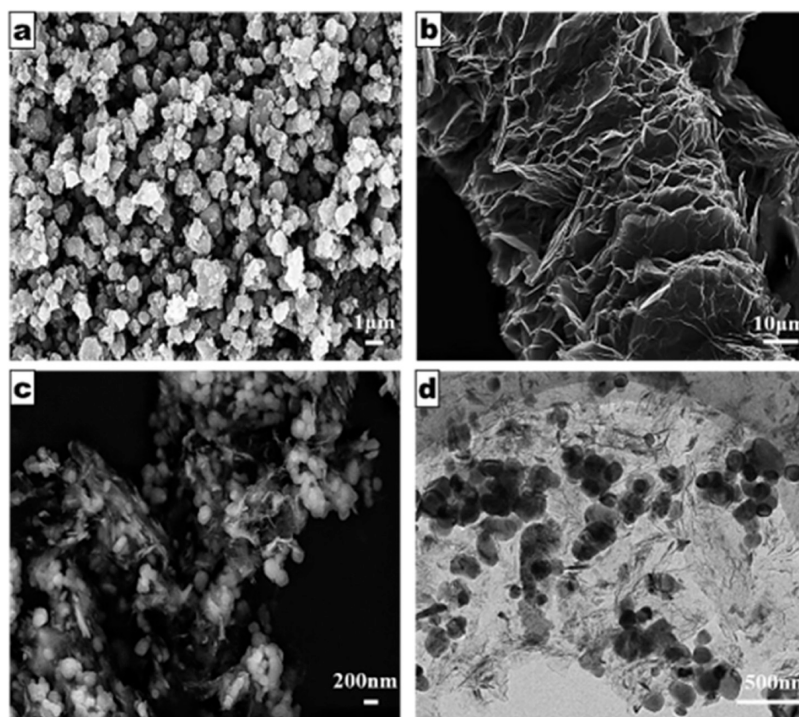
Figure 3. SEM images of (a) TiO_2, (b) expanded graphite, and (c) MGTC and (d) TEM image of MGTC.

2. CHARACTERIZATIONS

2.1. Materials. Expanded graphite was prepared by heating unexpanded graphite in an electric chamber furnace equipped with a 4 kW power source. The unexpanded graphite was heated to 1000 °C and maintained at that temperature for 20 min. The expanded graphite was obtained after cooling the product to room temperature. Unexpanded graphite was obtained from Shanghai Yifang Graphite Co., Ltd. TiO_2 nanopowders (99.9%, 1 μm) were purchased from Xilong Chemical Co., Ltd. Oleic acid (99%) was purchased from Sinopharm Chemical Reagent Beijing Co., Ltd. No further purification was performed on any of the chemicals.

2.2. Preparations of MGTC Lubricating Additive. The preparation process for obtaining the graphene-supported titanium dioxide nanocomposite lubricant additive (MGTC) is shown in Figure 1. Using plasma-assisted high-energy ball milling equipment, with oleic acid as the wet grinding medium and modifier, 1 g of expanded graphite/4g TiO_2 and 500 mL of oleic acid solution were mixed ultrasonically and evenly and placed into a tank to effect the plasma-assisted high-energy ball milling, which was conducted for 10 h. The main parameters of the procedure are as follows: the discharge voltage was 22 kV, the vibration frequency of the ball mill is 16 Hz, the amplitude was 10 mm, and the ball mill tank was filled with 0.1 MPa atmospheric environment. Using petroleum ether as the extraction agent, the prepared mixed solution of oleic acid-

modified graphene and titanium dioxide was shaken evenly with petroleum ether and then placed into a centrifuge tube. Centrifugation was conducted repeatedly at a centrifuge rate of 4000 r min^{-1} until the color of the upper petroleum ether solution was clear and transparent after extraction. The extracted precipitate was dried at 90 °C for half an hour in a drying box to produce the powder product.

2.3. Techniques. To determine the chemical composition of the materials, Fourier transform infrared (FT-IR) analyses were conducted on the experimental materials (NICOLET IS10, Thermo NICOLET) in the range from 500 to 4000 cm^{-1}. In addition, X-ray powder diffraction analysis of the materials (MiniFlex600, Rigaku) was used to characterize their crystal structure. The anode target was Cu with a Kα line (λ = 1.5406 Å), and the scanning angle ranged from 10 to 90° of 2θ, with a scan speed of 10° min^{-1}. The physical characteristics of MGTC were analyzed using a confocal Raman spectrometer (Horiba, HRE) with an argon ion laser at 532 nm. The microstructure of the powders was characterized by transmission electron microscopy (HRTEM, TECNAI G230S-Twin, Hillsboro) and scanning electron microscopy (FESEM, ZEISS VEO 18). Tribology experiments were performed on a MMW-1A four-ball friction and wear testing machine. The steel balls used in the ball milling were composed of E-52100 nickel−chromium alloy steel with a diameter of 12.7 mm, a Rockwell hardness of 64−66, and roughness Ra = 0.02,
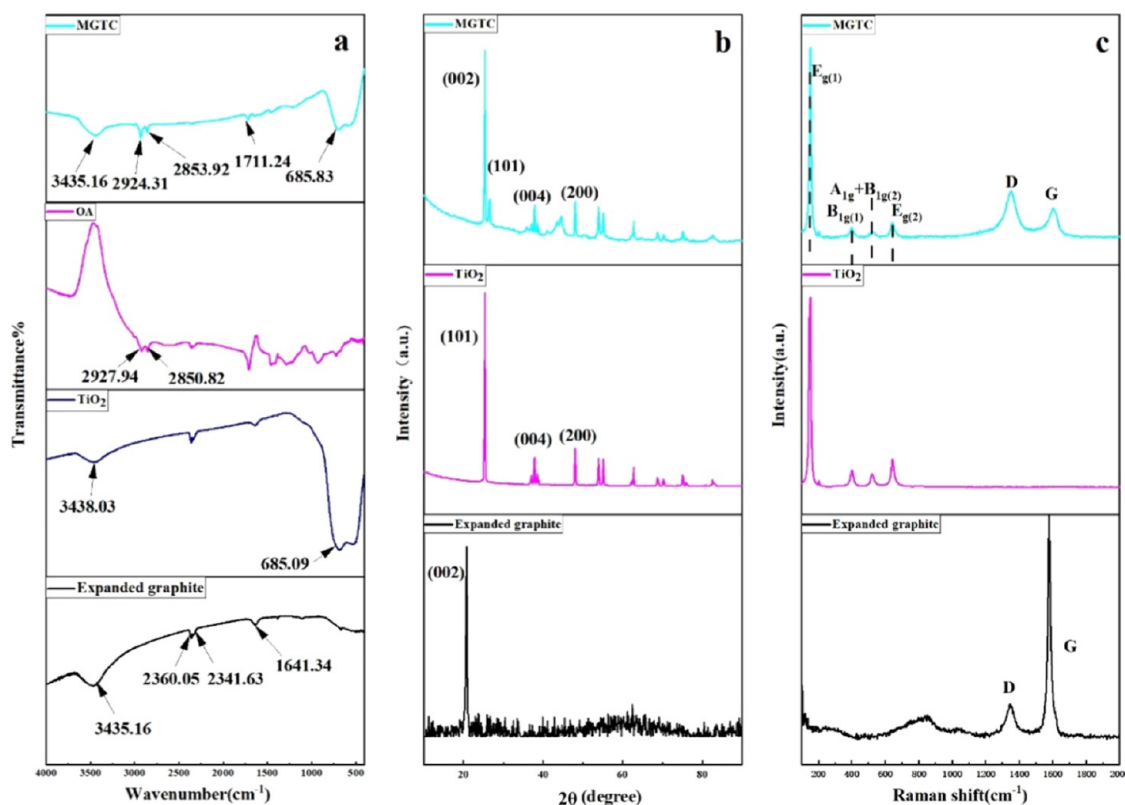
Figure 4. (a) FT-IR spectra; (b) X-ray diffraction (XRD) patterns; and (c) Raman spectra of MGTC, TiO_2, and expanded graphite.

following the American Iron and Steel Institute standard. Three clamped steel balls form a three-point contact cavity which is forced through the head ball with a force of 392 N at 75 °C and rotated for 60 min at 1200 r min^{-1}. The anti-wear performance of the oil samples was determined by averaging the diameters of three steel balls in the bottom clamp. The diameter and surface morphology of the steel ball were measured by scanning electron microscopy (ZEISS VEO 18) and three-dimensional (3D) morphology analyzer (KEY-ENCE). X-ray energy spectrum analysis (SU8010, HITACHI), Raman spectroscopy (Horiba, HRE), and X-ray photoelectron spectroscopy (Thermo Fisher Science) were used to analyze the chemical composition and valence states of the worn surfaces.

A laboratory bench scale friction test was conducted on the material using the piston ring and cylinder liner material of a MAN B&W 6S42MC7 diesel engine. A reciprocating sliding arrangement was used to simulate the contact between the piston ring and its mating liner near the top dead center position in the cylinder, where liquid lubrication is adequate, but most metallic wear is known to occur. The piston ring and cylinder liner samples used in the experiment were uniformly cut from the diesel engine's cylinder liner and piston ring, as shown in Figure 2. Prior to performing the wear experiment, the cylinder liner was run-in with the piston ring sample, and this sample was cleaned with absolute ethanol and in an ultrasonic cleaner. The stroke was set at 10 mm, and the frequency was 10 Hz. The test was conducted at room temperature by applying a load of 160 N during oscillation. The friction test was conducted for 60 min.

3. RESULTS AND DISCUSSION

3.1. Morphology and Structure of Expanded Graphite, TiO_2, and MGTC. The DBDP process reduces the thermal explosion and pulse electron bombardment effects, resulting in a rapid reduction in the time required to peel apart the graphite. The high electron density and energy of the DBDP process can produce bond breakage in some polymers and polymerization in others, which facilitates the formation of the MGTC nanocomposite powder. Figure 3 shows SEM and TEM images of nano TiO_2, expanded graphite, and MGTC. Titanium dioxide (TiO_2) powder is shown in Figure 3a and appeared to exhibit an average particle size of 1 μm. The SEM photograph of expanded graphite is shown in Figure 3b. The expanded graphite is wormlike and has numerous folds and gaps between the lamellar, which can be conducive to the attachment of graphite glass and TiO_2 nanoparticles. As shown in Figure 3c, TiO_2 was attached to graphene after plasma-assisted ball milling for 10 h. Multilayer graphene was evenly coated with TiO_2 particles, forming a good three-dimensional composite shape. It is evident from the measurements that the primary particle size of TiO_2 was reduced from about 1 μm to about 150 nm, and the effect of this reduction in size is quite apparent. This work was conducted by ball milling expanded graphite and nano TiO_2 in the same water solution. During ball milling, freshly peeled graphene was unstable and tended to adhere to the refined nano TiO_2 particles and roll on them. Images representing the TEM images of MGTC composite material are shown in Figure 3d. As can be seen, the nano TiO_2 material exhibited a regular spherical shape, and the surface was coated with multilayer graphene. These images directly reflect the microscopic morphology of the MGTC composite materials.
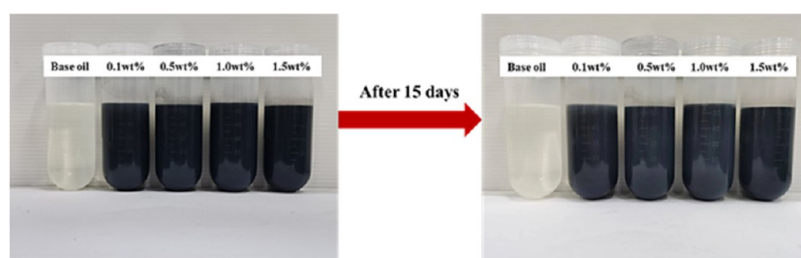
Figure 5. Photos of different dispersions for just-prepared and after 15-day storage.
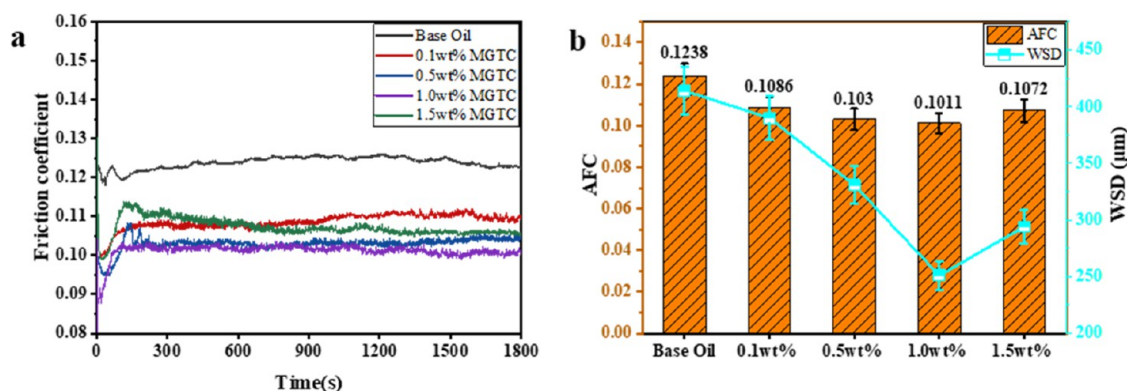
Figure 6. (a) Friction coefficients; (b) average friction coefficient (AFC), and wear scar diameter (WSD) of the wear scars lubricated by base oil and 0.1, 0.5, 1.0, and 1.5 wt % compound oil.

Figure 4a shows the FT-IR images of the nanopowder. The expanded graphite exhibited an absorption peak at 3435.16 cm^{-1}, which was attributed to the stretching vibration peak of −OH groups. The absorption peaks at 2360.05 and 2341.63 cm^{-1} were the result of CO_2 in the ambient air during the experiment. It is a structural characteristic of expanded graphite to exhibit the stretching vibration peak of C═C at 1641.34 cm^{-1}. It should be noted that TiO_2 has a height broadening peak at 685.09 cm^{-1}, which is caused by an oscillating absorption peak formed by the Ti−O bond of the octahedron. As shown in the FT-IR spectra of MGTC nanocomposites, several new absorption peaks were observed at 2924.31 cm^{-1} (−CH$_2$), 2853.92 cm^{-1} (−CH$_3$), 1711.24 cm^{-1} (−CH═CH−). The presence of these peaks demonstrates that the nano TiO_2 recombined on the graphene, while the oleic acid was modified it in situ.

As seen in Figure 4b, expanded graphite has a diffraction peak (002) at 25.08°, suggesting a high degree of crystallinity and a very well-stacked, layered structure. The JCPDS no. 78-2486 card with lattice constants $A = 3.784$ Å, $B = 3.784$ Å, and $C = 9.514$ Å was used to calibrate the diffraction peaks of anatase TiO_2.[21] Unlike the characteristic peaks of nano TiO_2, the characteristic peaks of MGTC became shorter with time, indicating that the number of layers and the grain size of the graphene decreased to some degree. The amorphous structure band centered on $2\theta = 25.37°$ is the characteristic peak of TiO_2(101). The diffraction peak (002) was then shifted to $2\theta = 25.22°$ as a result of this TiO_2 being grafted onto graphene. According to Bragg's Law ($2d \sin \theta = n\lambda$), it was found that the crystal plane spacing increased when the TiO_2 matrix was grafted onto graphene.[22]

Figure 4c shows the Raman spectra of expanded graphite, TiO_2, and MGTC nanocomposites. The Raman spectra of the expanded graphite samples showed two prominent characteristic peaks at 1350.1 and 1580.6 cm^{-1}, corresponding to D and G peaks.[23] It has been determined that peak D peak represents disordered sp^2 carbon, while peak G is indicative of orderly sp^2 hybrid vibrations. The ratio of peak D to peak G (I_D/I_G) can be used to evaluate the degree of defects in a carbon material. An increase in the I_D/I_G ratio indicates that the ordered sp^2-hybrid carbon atoms in the carbon material are reduced, and there is an increase in the defects in the material. The Raman vibration mode of anatase TiO_2 is $A_{1g} + 2B_{1g} + 2E_g$, as shown in Figure 3c. The four characteristic peaks at 149.6 cm^{-1} ($E_{g(1)}$), 399.4 cm^{-1} ($B_{1g(1)}$), 514.1 cm^{-1} ($A_{1g} + B_{1g(2)}$), and 640.4 cm^{-1} ($E_{g(2)}$) were the characteristic Raman peaks of anatase TiO_2.[24] Compared with the TiO_2 Raman spectra, the characteristic peaks of MGTC at 149.6, 406.1, 517.1, and 647.2 cm^{-1} were consistent with those of anatase TiO_2. This again confirmed the presence of the TiO_2 anatase phase in the MGTC. In addition, the Raman spectra of the MGTC composite exhibited peaks that were characteristic of carbon at the positions of 1356.8 cm^{-1} (D peak) and 1601.8 cm^{-1} (G peak). After calculations, the I_D/I_G ratio of MGTC was calculated to be 1.64, while the I_D/I_G value of the original expanded graphite was only 0.15, indicating that the plasma-assisted ball milling process had resulted in the intercalation of titanium dioxide. Also, the mechanical peeling in the high-energy ball milling process quickly peeled the structure of the expanded graphite into a multilayer graphene. These results confirm the presence of TiO_2 nanocomposite powder reinforced with multilayer graphene.

To evaluate the dispersion stability of MGTC nanopowders in a base oil at different concentration levels, 0.1, 0.5, 1.0, and 1.5 wt % of MGTC nanoparticles were ultrasonically dispersed in the 500 N base oil until no residual solids were detected. As shown in Figure 5, after 15 days of storage, the dispersed MGTC powder in the base oil at different concentrations appeared to still be evenly dispersed. This result indicates that

MGTC nanoparticles enjoyed good dispersion stability in the base oil.

3.2. Tribological Performance Analysis. Using the ASTM D4172-21 lubricating oil anti-wear and anti-wear test method (four-ball method), the friction coefficient and wear scar diameter of steel balls in the experimental composite oils were investigated to ascertain the tribological properties of the composite oils. Figure 6a shows that the MGTC nano-lubricating oil additive significantly reduced the composite lubricating oil friction coefficient compared to the base oil. Compared to the base oil, the average friction coefficient decreased to 0.1011 when 1.0 wt % of MGTC was added to the base oil. This occurred because the base oil cannot provide an evenly lubricated surface during pair contact, so the surfaces of the steel ball pairs are in direct contact, and the friction coefficient rises rapidly. As a result of its synergetic friction coefficient, the MGTC composite nanolubricating oil additives reduced the friction coefficient in the wear region by reducing direct contact between the friction pair and by filling the wear area with graphene and titanium dioxide.[25]

While the coefficient of friction decreased slightly following addition of the additive, addition of 1.5 wt % of the additive actually resulted in a slight increase in the coefficient of friction. The primary reason for this was that more abrasive particles were introduced onto the pair surfaces when excess nano TiO_2 was added. Furthermore, we examined the diameter of wear scars on the steel ball's surface as well as the amount of additive added after the friction test was completed. It can be seen from Figure 6b that the relationship between the amount of MGTC added and the coefficient of friction of the various oils was telling. It was found that the composite oil's anti-wear and antifriction properties were significantly improved by addition of the additive, and the wear scar diameter decreased significantly after adding the additive. Based on these data, a 1.0 wt % addition of the additive appeared to improve antifriction and wear reduction, mainly because the additive provided a uniform layer of protection to steel balls. By adding nanometer-sized lubricating oil additives to the cylinder liner and piston ring, a uniform continuous oil film was generated that reduced the contact friction between the friction pair as could occur on the engine surfaces in ship diesel engines.[26] MGTC's oil additives reduce contact friction between friction pair and surface in the process. It reduces viscous friction caused by interlayer shear of lubricating oil by acting as ball bearings within MGTC composite nanolubricant additives. It has been demonstrated that MGTC nanolubricant additives can improve engine performance and reduce engine friction loss to a significant degree.

Using the ASTM D2783-21 lubricant carrying capacity determination method (four-ball method), this study evaluated the carrying capacity of liquid paraffin additives in composite oils. The results of these evaluations are shown in Figure 7. It can be seen that the P_B value of base oil without the addition of products was 475 N. The P_B values of the liquid paraffin begin to increase following addition of 1.0 wt % of the additive, where the P_B values reached 653 N, which was 37.5% higher than the value for the base oil. There has been great progress in improving the carrying capacity of composite oils by adding nanometer lubricating oil additives. To accomplish this, the additive must form a boundary lubrication layer that separates the friction surfaces to lower the friction between the steel ball surfaces.[27] This is an example of the effect of surface
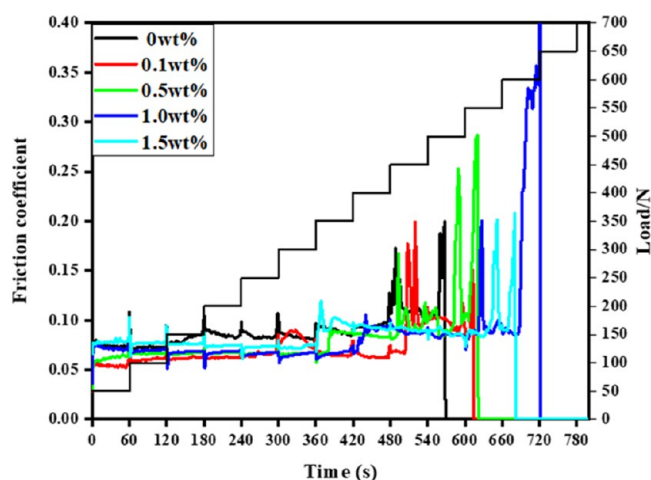
Figure 7. Maximum nonclamping load of each oil sample.

modification on the bearing capacity of the base oil, although this has also been demonstrated in the composite oil.

Figure 8a illustrates the micrographs of KEYENCE after a 60 min friction test before and after addition of the subject nanoparticles. The maximum diameter of the spot during the friction test was 414 μm when the base oil was lubricated. As shown, addition of the nanoparticle additive resulted in a significant decrease in the diameter of the spot and the surface roughness of the spot. The 1.0 wt % compound oil produced the smallest spot diameter after addition of nanoparticles. Compared to the base oil, the composite oil resulted in a decrease of 39.37%, as shown in Figure 8d. There was a synergistic effect observed between the TiO_2 particles and graphene in the oil, and the oil exhibited better lubrication properties than the pure base oil. This was because the added nanoparticles can coat the friction pairs and act as micro bearings, which redirects the contact sliding friction of the matrix materials of the friction pair into rolling sliding mixed friction, thereby reducing friction and wear.[28] Due to the granular nature of nano TiO_2, the diameter of the friction spot grew as the content of the additive in the oil increased. Nano TiO_2 can act as both micro bearings and as abrasive particles in the friction pair, which produced an increase in the diameter of the friction spot when the content was very high. It has been demonstrated that certain additives can have a significant impact on reducing the friction coefficient of a surface. However, excessive additive content can increase the depth and width of wear and scratches over time.

The four-ball friction testing machine encompasses the use of three friction balls, the ball is retained in the chuck, the ball group is fixed, and the ball is in contact with the ball group. A spindle drives the upper ball to rotate, and a loading system loads the lower ball. By analyzing the forces exerted by the upper ball on the lower three balls at three contact points, the forces of the four steel balls can be expressed as an equilateral tetrahedron, as shown in Figure 9. Suppose the vertical load F is loaded on the top ball

$$F_1 = F_2 = F_3 = 0.4082F \qquad (1)$$

The distance between the contact point of the head ball and the bottom ball and the perpendicular line of the center of the head ball O_1B_1, O_1C_1, O_1D_1, to obtain the linear velocity of the head ball at the contact point. From the geometric relationship in the figure
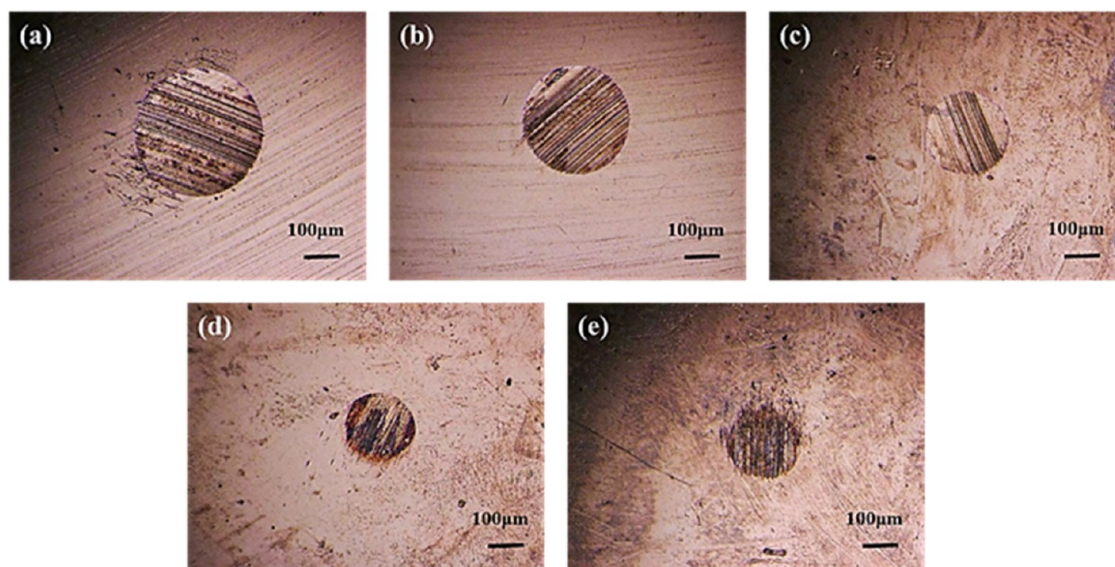
Figure 8. Microscope images of steel ball surface after friction test of compound oil samples with different additive amounts by four-ball method: (a) base oil; (b) 0.1 wt %; (c) 0.5 wt %; (d) 1.0 wt %; and (e) 1.5 wt %.
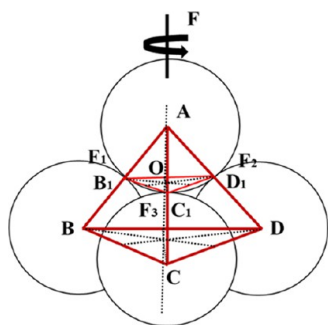
Figure 9. Stress analysis diagram of steel balls of the four-ball machine.

$$OB_1 = 1/\sqrt{3}\, R_1 = 0.5774 R_1 \tag{2}$$

Then, the linear velocity of the ball at the contact point is

$$U = 2\pi R \times 1200 \times 10^{-3}/60 G^* = \alpha E' \tag{3}$$

$$E' = E/(1 - \nu^2) \tag{4}$$

$$U^* = \eta_0 U/E' R_x \tag{5}$$

$$\eta_0 = \nu_0 \rho \tag{6}$$

$$F^* = F_1/E' R_x^2 \tag{7}$$

Based on the elliptic contact viscoelastic theory of Hamrock-Dowson,[29,30] the central oil film thickness h_c was calculated by measuring the dynamic viscosity of different composite oils so as to analyze wear reduction properties and anti-wear properties.

$$h_c = 2.69 R_x U^{*0.67} G^{*0.53} F^{*-0.067} \times (1 - 0.6/e^{-0.73k}) \tag{8}$$
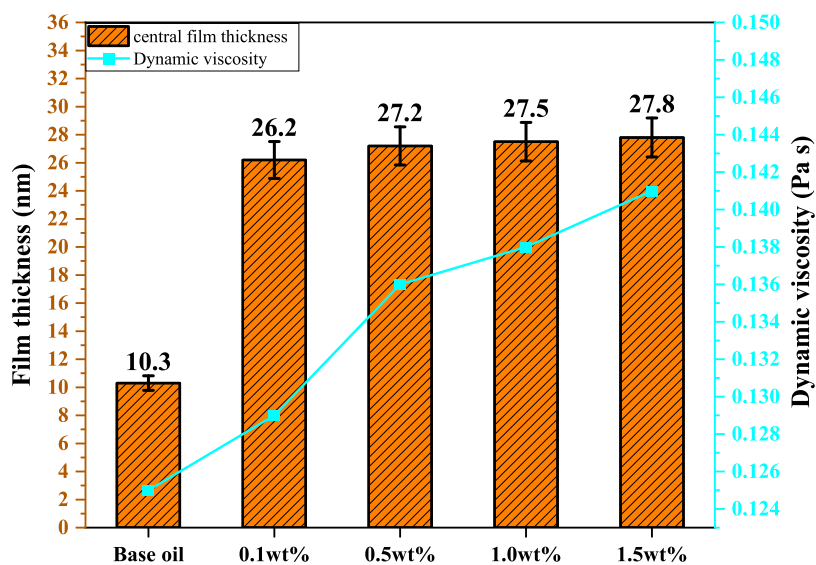
Figure 10. Dynamic viscosity and central oil film thickness of different composite oils.
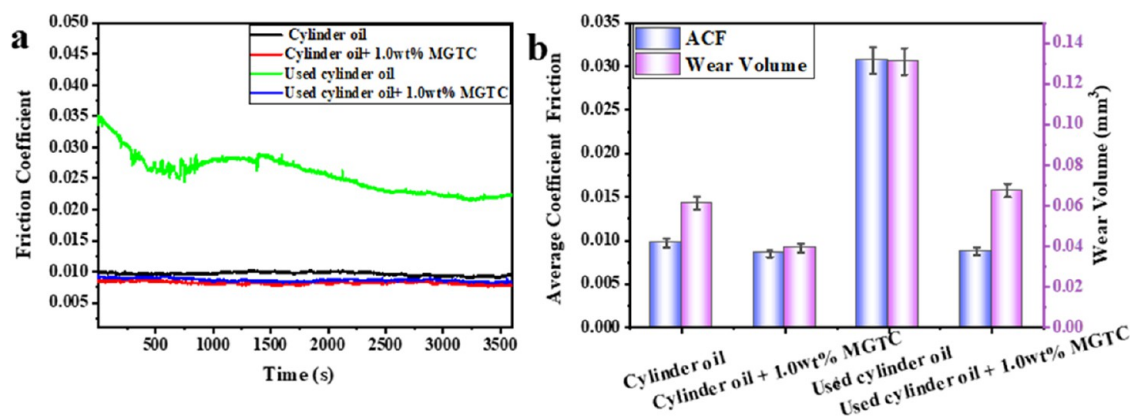
Figure 11. (a) Friction coefficients; (b) average friction coefficient (AFC) and wear volume of the piston ring and cylinder liner lubricated by base oil and 0.1, 0.5, 1.0, and 1.5 wt % compound oil.

where R is the radius of the steel ball; U is the linear speed of steel ball; F_1 is the applied force on the bottom ball contact surface; ν is the Poisson's ratio of the steel ball; E is the elastic modulus of steel ball; E'' is Young's modulus of steel ball; η_0 is the dynamic viscosity of lubricating oil; α is the pressure viscosity coefficient of lubricating oil; and K is the coefficient,

$$k = 1.03\left(\frac{R_y}{R_x}\right)^{0.64}.$$

Figure 10 shows the central oil film thickness and dynamic viscosity of the composite oil samples with various additive amounts. As shown in Figure 10, after the addition of nanopowder to the base oil, both the film thickness and dynamic viscosity of the oil were considerably increased. The oil film thickness and dynamic viscosity increased by 164 and 8.8% compared to the base oil when the additive amount was increased from 0 to 0.5 wt %. There was no significant increase in the oil film thickness or dynamic viscosity when the amount of additive was increased from 0.5 to 1.5 wt %. These parameters increased by 2 and 3.7% but gradually stabilized when the amount of additive was 1.5 wt %. These results indicate that addition of the MGTC nanopowder to the base oil can substantially enhance the oil film thickness and dynamic viscosity. When the optimal amount of the additive was attained, the central oil film thickness tended to stabilize. The top and bottom TDC states in the working cycle of a diesel engine are referred to as boundary lubrication states. During the lubrication process, the micro-convex body's lubrication film thins and easily breaks down.[31] At this point, the friction coefficient is the highest, and the friction loss is the largest. With the addition of MGTC nanopowder to the base oil, the dynamic viscosity of the base oil can be significantly increased while the oil film thickness is also greatly improved.[32] In addition to this, the TDC and boundary lubrication state of the diesel engine are significantly improved, wear power consumption is reduced, and the engine's service life is prolonged.

3.3. Tribological Experiment of Cylinder Liner Piston Ring. The efficiency and fuel economy of diesel engines is affected, in part, by the friction that occurs between the moving parts in the engine. A substantial portion of the friction losses in such engines occurs at the interface between the rings and liners. Consequently, a reciprocating sliding arrangement was used to simulate the oscillating contact between a piston ring and its mating cylinder bore surface near the top dead center position in the cylinder. This is the area where the most

severe surface contact conditions occur. Engine oils are in thermal, chemical, and lubricating contact for most of their working life. Under these conditions, the oil ages, which changes its viscosity, atomic weight, solids content, acidity, and chemistry. The friction test of the piston ring and cylinder liner in a new oil cannot fully reflect the working conditions of a diesel engine. However, additive-depleted, used oil can produce high wear and corrosive attack on engine parts. We obtained fresh FEOCY 54 (SAE 50 cylinder oil for use in engine model MAN B&W 6S42MC7), as well as old cylinder oil used for 38 611 h of normal operation. MGTC nano-lubricating additive was added to the used cylinder oil, and tribological experiments were conducted for 1 h before and after the oil was added. A bench friction test was conducted to verify MGTC's wear reduction and anti-wear properties.

It can be seen from Figure 11a that the friction coefficient of the used cylinder oil was approximately 0.0307, and it exhibited a trend of continuous fluctuation. After 30 min of testing, the friction curve exhibited an initial decrease in friction coefficient and then an increase. The latter was caused by the accumulation and agglomeration of iron filings and dust particles produced during the test. The lack of lubricant caused the friction coefficient to greatly fluctuate. When 0.1 wt % of MGTC particles was added, the friction coefficient was significantly reduced and the test curve was relatively stable, with the friction coefficient reduced by 72%. This was the result of the nanoparticles entering the frictional contact zone, transforming the sliding friction into rolling friction. The MGTC particles deposited on the cylinder liner surface also reduced the generation of abrasive wear, thus reducing friction. The friction curve of the unused cylinder oil with 1.0 wt % MGTC lubrication additive is shown at the bottom of the figure, which was lower than that of fresh cylinder oil, indicating that the addition of the MGTC lubrication additive can significantly improve the lubrication performance of Marine grade cylinder oil. Figure 11b shows the oil samples' average friction coefficient and wear volume. The average friction coefficient of the used cylinder oil with 1.0 wt % MGTC was 0.0087, and the friction coefficient and wear volume were reduced by about 72 and 48.5%, respectively, when compared to the used cylinder oil that lacked the lubricant additive. However, the average friction coefficient and wear volume of the fresh cylinder oil with 1.0 wt % MGTC composite lubrication additive were reduced by 12.4 and 36.1% compared with the lubricant that lacked the additive. In
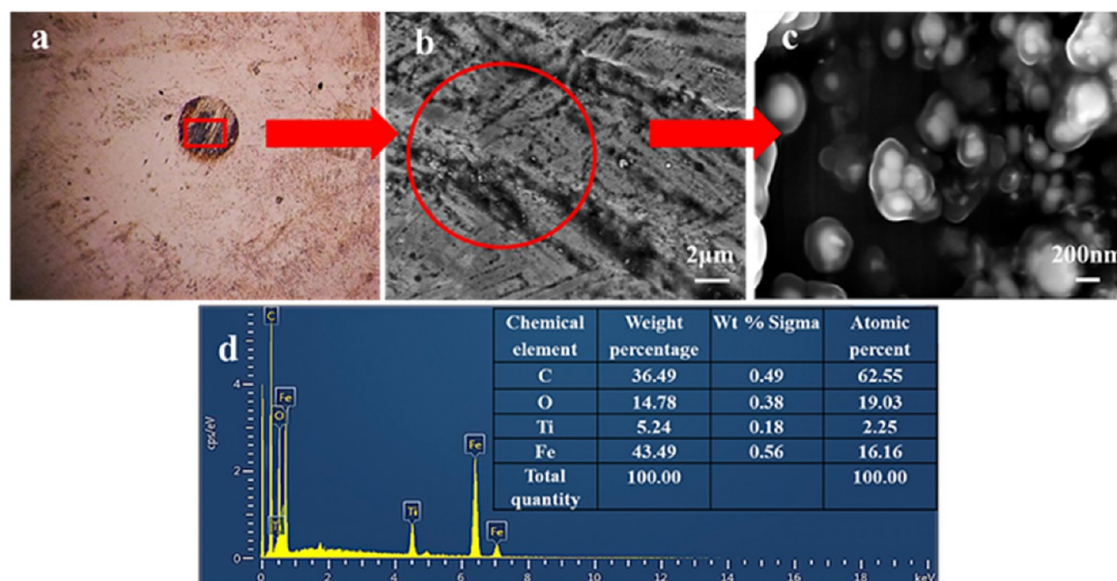
Figure 12. Optical micrograph of the rolled surface (a); SEM (b, c); and energy-dispersive spectrometry (EDS) images (d) of steel ball spots after friction test with 1.0 wt % compound oil.
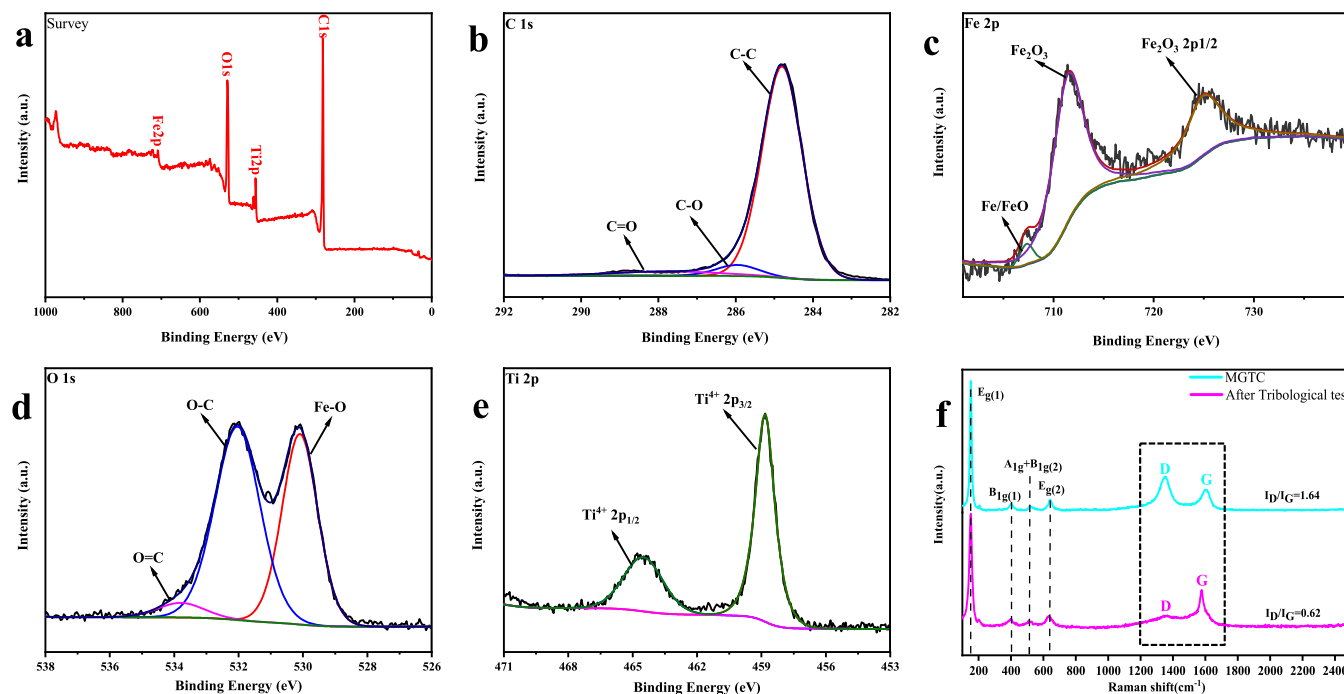
Figure 13. XPS energy spectrum on the rolled surface of (a) survey, (b) C 1s, (c) Fe 2p, (d) O 1s, (e) Ti 2p, and (f) Raman image of steel ball spot after friction test with 1.0 wt % compound oil addition.

general, MGTC composite lubrication additive appeared to improve the lubrication ability of Marine grade cylinder oil, offering excellent anti-wear behavior that can significantly improve the tribological performance of the cylinder liner piston ring.

3.4. Surface Analysis of Friction Pair. Microscopic analysis was conducted on the surface of the grinding spot of the friction pair for the 1.0 wt % MGTC oil addition (as shown in Figure 12). The diameter of the grinding spot measured by the microscope was 251 μm, which was the smallest in all of the tests (Figure 12a). This was due to the lamellar structure of nano TiO_2 and multilayer graphene. With a relative movement

of the friction pair, the lamellar graphene structure slips due to the weak binding force between graphene lamellae. The graphene lamellae attached to the friction pair can protect the contact surface from wear. As can be seen from Figure 12b, nano TiO_2 particles will deposit on the surface of the friction pair to repair the worn surface while playing the role of micro bearing. From a macro perspective, nano TiO_2 can effectively reduce friction and wear due to its micro bearing role, and the ultimate performance is the minimum wear in the presence of 1.0 wt % MGTC addition to the oil.

Figure 12c shows the SEM image of the surface of the friction pair after a 60 min tribology experiment with 1.0 wt %
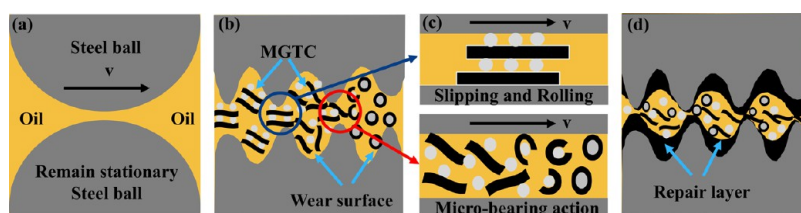
Figure 14. Lubrication mechanism of nanoadditive: (a) relative motion of friction pair; (b) interlamellar slip of multilayer graphene and TiO$_2$ particle rolling; (c) MGTC's slipping and rolling and micro bearing action, and (d) repair of worn surfaces.

MGTC additive level in the oil. Compared to the MGTC nanopowder prepared in Figure 3c, the composite powder appears to be peeled off into a core−shell structure after the friction test, which substantiates the rolling sliding wear reduction mechanism of the MGCT lubricant additive during lubrication. With the addition of 1.0 wt % MGTC, the dynamic viscosity of base oil increased from 1.25×10^{-2} to 1.38×10^{-2} Pa s. More MGTC nanoadditives were filled and deposited on the friction pair's surface as a result of the rise in dynamic viscosity, which also increased the oil film thickness of the composite oil. In solid−liquid mixtures, friction pairs of high-speed mechanical movement in the form of lubrication film pressure wave moves back and forth, and in the inlet and outlet formed on the friction pair's surface, pressure gradients are formed under the pressure of the contact layer. Loss of TiO$_2$ leads to the stripping of multilayer graphene and can also draw on the spherical structure of nanometer TiO$_2$ balls.[7] The lubricating oil flows on a metal surface as a result of siphoning. On sliding surfaces, the siphoning is induced by friction, so the MGTC's multilayer graphene sheets can rapidly recombine, which will reduce the run-in period. In addition to changing the form of contact between the friction pairs, the nanoparticles can also discharge tiny abrasive metal particles through the gap between friction pairs, which will scratch the surface of friction pairs during the process.[33] As a result, friction surface stripping of graphene occurs during the formation of the deposited film, preventing abrasive wear (Figure 12c). Despite this, the combination of nanoparticles and abrasive particles between friction pairs does not prevent the nanoparticles from acting like micro bearings, effectively reducing friction and wear.[34] The EDS spectrum of the steel balls is shown in Figure 12d, where it can be seen that Ti, C, O, and other elements were present on the surface of the friction pair, suggesting that the MGTC powder formed a deposition film on the surface of the friction pair to avoid direct pair contact.

To further understand the improvement of the friction performance and lubrication mechanism of the MGTC additive, X-ray photoelectron spectroscopy (XPS) was used to determine the elements and their chemical states on the wear surface that had been lubricated with 1.0 wt % additive in the oil. The results are shown in Figure 13. An external pollution carbon source with a binding energy of 284.8 eV was used as the benchmark for the high-resolution spectrum. Peak fitting was performed using the XPS PEAK software, and high-resolution spectra analysis for elements C, O, Ti, and Fe was conducted, as shown in Figure 13a−e. Figure 13a shows the full spectrum of XPS on the surface of the abrasive spot after the tribology experiment. It can be seen that the surface of the abrasive spot contains the characteristic elements C, O, Ti, and Fe. The C 1s peaks can be divided into three sub-peaks (284.8, 286.3, and 288.5 eV), corresponding to the different chemical

binding modes of C element [C−C, C−O, and C=O],[35] indicating the formation of physical/chemical adsorption films on the sliding interface. For the O 1s signal, there are three characteristic peaks at 529.7, 531.3, and 532.9 eV, respectively, which can be attributed to iron oxide and carbon oxide (Fe−O, C−O, C=O).[36] The valence state of iron is an important factor to understand to explain the adsorption interaction during the formation of the lubricating film. From the signal of Fe 2p, it can be seen there are signal peaks for the metal Fe/FeO, Fe$_2$O$_3$, and Fe$_2$O$_3$ 2p$_{1/2}$ at 706.8, 711.8, and 725.6 eV for the MGTC nano lubricated spot surface.[34] These results indicate that the MGTC additive was adsorbed on the metal surface and formed an effective adsorbed lubricating film on the friction interface.

The wear surface of the 1.0 wt % MGTC nanoadditive was analyzed by Raman spectroscopy, as shown in Figure 13f. It can be seen from Figure 13f that the Raman spectrum of friction surface was similar to that for the MGTC. The D band at 1351.7 cm^{-1} and the G band at 1605.6 cm^{-1} are the characteristic peaks for carbon, demonstrating the presence of a graphene deposition coating on the friction pair's surface.[37] Further observation showed that four characteristic peaks were observed in the Raman spectra of MGTC at 152 cm^{-1} (E$_{g(1)}$), 402.2 cm^{-1} (B$_{1g(1)}$), 512.1 cm^{-1} (A$_{1g}$ + B$_{1g(2)}$), and 641.4 cm^{-1} (E$_{g(2)}$).[38] In the Raman spectra of carbon-based materials, the parameter I_D/I_G is a vital index to characterize the defect level. As shown in Figure 10f, the I_D/I_G value of the original MGTC powder is greater than 1, indicating that the carbon layer structure has been destroyed and the amorphous structure has formed.[39] In addition, the I_D/I_G of MGTC decreased from 1.64 to 0.62, indicating that a sp^2 hybrid into dominant similar transfer graphene film formed on the friction pair's surface due to the friction heat generated and contact pressure exerted during the friction process.[40−43] Due to the presence of titanium dioxide, the composite powder showed higher structural stability. Graphene exhibited fewer structural defects during friction testing.

Combined with the above tribological experiments and analysis of the micro-morphology of the friction spot, it appears likely that after the granular nano TiO$_2$ particles entered the friction pair, some of them played the role of micro bearings. Following this, the material was discharged by the rotation of the friction pair and did not participate in the chemical reaction with the surface materials of the friction pair. The other part of the compressed micro-nanoparticles probably filled the pits and damaged parts on the workpiece surfaces, which was equivalent to reducing the surface roughness of the actual contact area and contact position, effectively playing a repair role. Moreover, the strong oxidizing capability of titanium dioxide probably helped to oxidize the friction surface of the steel ball, forming a layer of chemical oxide, which helped reduce friction and wear more effectively.
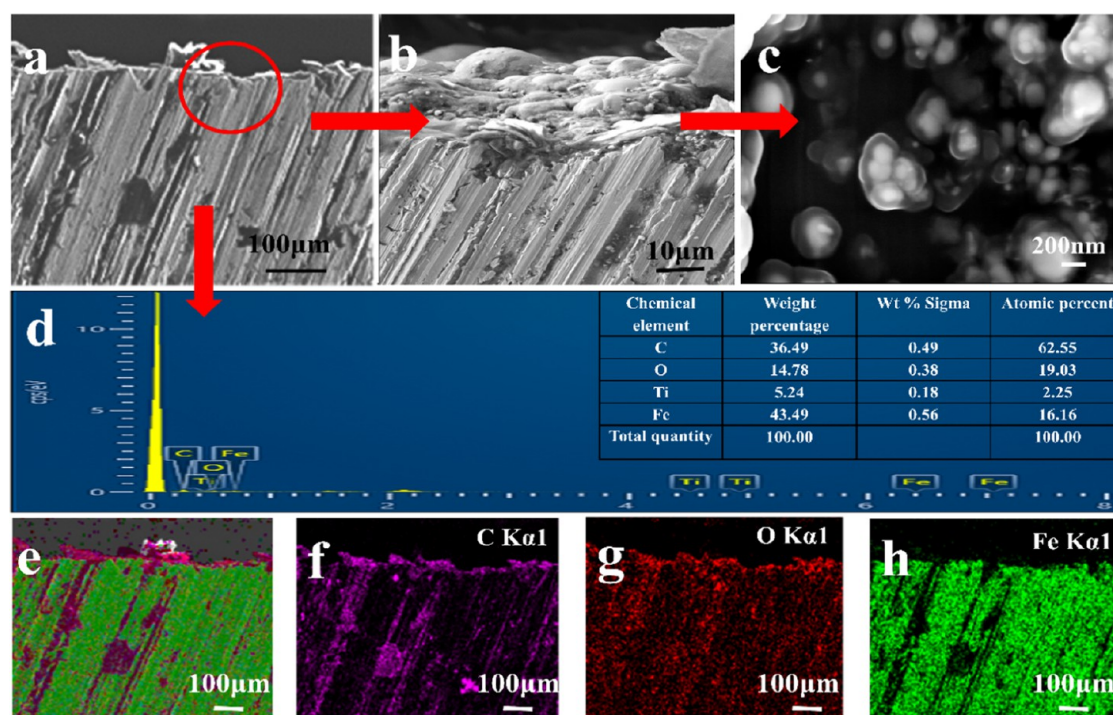
Figure 15. (a) Image of the protective film formed on a wear scar lubricated by 1.0 wt % MGTC compound oil. (b, c) Image of the protective film. (d–h) EDS mapping of wear scar and EDS mapping of C, O, and Fe.

Due to the lamellar graphene's poor interfacial adhesion, it slides during the rotation of the friction pair, and some very thin graphene lamellar graphene can be attached to the friction pair's matrix material to play a part in healing the worn surface.

4. FRICTION MECHANISM ANALYSIS

Based on the results shown in Figure 11, it can be seen that the modified MGTC material dispersed well in low-polarity organics such as liquid paraffin. The MGTC dispersed in oil is easily deposited on the surface of steel balls due to high-speed sliding between the friction pairs (Figure 14a), which fills in the creases on their surfaces. TiO_2 and graphene are relatively active materials. The surfaces and grooves of the steel balls can be covered with a protective layer of these active materials during the friction process to protect the surfaces of the steel balls. Nanoparticles have a relatively short retention time in the friction contact area, meaning they exit the contact area before the external load increases. This is equivalent to the ball rolling on top and further reduces wear. Nano MGTC enters into the friction pair with lubricating oil. Graphene and TiO_2 particles with different particle sizes can serve as micro bearings between friction pairs due to the uneven surfaces of microscopic friction (Figure 14b). This transforms a sliding friction process into a rolling sliding mixed friction process.

In contrast to pure base oil, the nano MGTC composite oil has small diameter particles and a smoother surface. The multilayer graphene particle structure plays a role as a micro bearing due to the weak interlamellar bonding (Figure 14c,d), which produces a very thin graphene layer between the friction pair surfaces and repairs the wear surface in the complex environment of high temperature and high pressure. Furthermore, the high oxidation capability of nano TiO_2 can help form metal oxides on the steel ball surface at high temperatures, which is another oxidation film layer that helps reduce friction and wear. In addition, the compressed nano and

microparticles can fill in the pits or damaged parts of the workpiece surfaces, which is equivalent to reducing the actual contact area and the roughness of the contact location's surface. The surface modification of graphene and TiO_2 effectively improves the dynamic viscosity of composite samples. Additionally, the adsorption effect of the powder surface carboxyl groups can increase oil film thickness, and the deposited nanoparticles produce a separate friction surface layer of an organic composite that alleviates friction. Spherical TiO_2 nanoparticles surrounded by multiple layers of graphene provide a lubrication film that is easy to shear (low coefficient of friction). The quasi-spherical shape of TiO_2 nanoparticles facilitates sliding shear between graphene sheets and sediments. Optimal tribological effects are achieved when TiO_2 + graphene + abrasive particle are used as a third body. This can be confirmed by the significant increase in the carrying capacity of the compound oil. Therefore, the composite oil containing the MGTC nanolubricant additive produces good antifriction and wear reduction performance.[44]

A cross section of the worn surface lubricated by the MGTC was examined using EDS and SEM after the tribological tests were completed. Figure 15 shows the results of the cross-sectional analyses. In Figure 15a,b, MGTC nanoparticles are shown in terms of their chemical composition and nanostructure. It was observed that the oxide layer structure had an approximate thickness of 1 μm. Figure 15c shows the nano ball effect of TiO_2 between the surface of the friction pair and the graphene sheet. Multilayer graphene is peeled off by the combined action of shear force and friction force, and the core–shell structure is formed by rolling TiO_2. The EDS element mapping in Figure 15d–h suggested that this tribo-film was rich in C, O, and Ti, which proves the existence of graphene and TiO_2 deposition films on the surface of the friction pair. Figure 13f shows the I_D/I_G of MGTC decreased from 1.64 to 0.62, indicating that an sp^2 hybrid into dominant

similar transfer graphene film formed on the friction pair's surface due to the friction heat generated and contact pressure exerted during the friction process. A synergistic effect was observed between nanoparticles of TiO_2 and multilayer graphene nanosheets when lubricated by MGTC nanocomposites, which was demonstrated by their ability to form films when symbiotically lubricated. It appears that addition of MGTC nanoparticles had a beneficial effect on the formation of an oxide layer and promoted the development of a tribo-film rich in C.

5. CONCLUSIONS

In this reported work, spherical TiO_2 was fixed onto multilayer graphene nanosheets (MGTC) by wet grinding and surface modification with oleic acid and plasma-assisted ball milling of the raw materials consisting of expanded graphite, a wet grinding medium, and anatase TiO_2. A variety of analyses, including XRD, FT-IR, Raman, XPS, SEM, and TEM were performed to characterize the morphology of MGTC nanocomposite oils. Tribological experiments were performed on the products and showed that addition of the MGTC composite nanoadditive significantly improved the viscosity and film thickness of the base oil and had better extreme-pressure wear resistance. The MGTC composite oil containing 1.0 wt % of the TiO_2 graphene composite additive exhibited good friction reduction and wear resistance, and the minimum diameter of wear spot on the test sample was 39.4% less than that using the base oil. The thickness of the oil film was 27.5 nm, which was 167% higher than the base oil. According to the analysis results of the surface of friction pair, the reasons for the improvement in the wear reduction performance exhibited by the MGTC nanocomposite versus the base oil were:

(1) After dielectric barrier discharge plasma-assisted ball milling for 10 h, the primary particle size of TiO_2 was reduced from about 1 μm to about 150 nm, and the effect of this reduction is quite apparent. As a result of the large number of fresh surface areas and crystal defects, the modifier bonded better to the surface of the nano TiO_2 powder. CH_2- and CH_3-oleophilic groups were grafted to the surface of MGTC to increase its dispersion stability in the base oil.

(2) With the addition of 1.0 wt % MGTC, the dynamic viscosity of the base oil increased from 1.25×10^{-2} to 1.38×10^{-2} Pa s. The long carbon chain modified on the surface of MGTC powder improved the dynamic viscosity of the composite oil samples and increased the thickness of the oil film on the surface of the friction pair. When the amount of additive in the oil was 1.0 wt %, the average friction system was reduced by 18.34% compared to the base oil. The abrasive spot diameter on the wear ball was reduced by 39.37% compared to the base oil. The extreme pressure anti-wear performance of the composite oil with 1.0 wt % MGTC was also significantly improved, and its PB value attained 653 N, which was 37.5% higher than the base oil.

(3) The slippage in the lamellar structure of multilayer graphene and the sliding shear of nano TiO_2 between the graphene lamellae cause the MGTC multilayer graphene additive to rapidly recombine on the surface of the friction pair as induced by friction, forming a third-body structure of TiO_2 + graphene + abrasive coated by multilayer graphene. The result is that the sliding friction

wear process between friction pairs is transformed into rolling friction to achieve the best tribological effect. At the same time, the MGTC attached to the surface of the friction pair reacts with the matrix material and oxygen of the friction pair under the complex environment of high temperature and high pressure and generates new substances on the surface of the friction pair to repair the worn surface.

■ AUTHOR INFORMATION

Corresponding Author

Le-yang Dai − *Fujian Provincial Key Laboratory of Naval Architecture and Ocean Engineering, School of Marine Engineering, Jimei University, Xiamen 361021, China;* orcid.org/0000-0003-4266-8925; Email: daileyang@jmu.edu.cn

Authors

Yu-kun Wei − *Fujian Provincial Key Laboratory of Naval Architecture and Ocean Engineering, School of Marine Engineering, Jimei University, Xiamen 361021, China*

Hai-chang Zhong − *Fujian Provincial Key Laboratory of Functional Materials and Applications, School of Materials Science and Engineering, Xiamen University of Technology, Xiamen 361024, China*

Hai-feng Liao − *Fujian Provincial Key Laboratory of Naval Architecture and Ocean Engineering, School of Marine Engineering, Jimei University, Xiamen 361021, China*

Xian-bin Hou − *Fujian Provincial Key Laboratory of Naval Architecture and Ocean Engineering, School of Marine Engineering, Jimei University, Xiamen 361021, China; College of Marine Technology, Beibu Gulf University, Qinzhou 535011, China*

Complete contact information is available at:
https://pubs.acs.org/10.1021/acsomega.2c05057

Notes

The authors declare no competing financial interest.

■ REFERENCES

(1) Syed, D.; Wani, M. Tribological Behavior of Chrome-Deposited SAE9254 Grade Steel Top Compression Piston Ring under Lubrication Starvation and Mild Extreme Pressure Lubrication. *Int. J. Engine Res.* **2021**, *22*, 1285−1300.

(2) Li, T.; Ma, X.; Lu, X.; Wang, C.; Jiao, B.; Xu, H.; Zou, D. Lubrication Analysis for the Piston Ring of a Two-Stroke Marine Diesel Engine Taking Account of the Oil Supply. *Int. J. Engine Res.* **2021**, *22*, 949−962.

(3) Sagin, S.; Madey, V.; Stoliaryk, T. Analysis of Mechanical Energy Losses in Marine Diesels. *TAPR* **2021**, *5*, No. 61.

(4) Singh, A.; Chauhan, P.; Mamatha, T. G. A Review on Tribological Performance of Lubricants with Nanoparticles Additives. *Mater. Today: Proc.* **2020**, *25*, 586−591.

(5) Wang, J.; Zhuang, W.; Liang, W.; Yan, T.; Li, T.; Zhang, L.; Li, S. Inorganic Nanomaterial Lubricant Additives for Base Fluids, to Improve Tribological Performance: Recent Developments. *Friction* **2022**, *10*, 645−676.

(6) Spear, J. C.; Ewers, B. W.; Batteas, J. D. 2D-Nanomaterials for Controlling Friction and Wear at Interfaces. *Nano Today* **2015**, *10*, 301−314.

(7) Wu, H.; Zhao, J.; Cheng, X.; Xia, W.; He, A.; Yun, J.-H.; Huang, S.; Wang, L.; Huang, H.; Jiao, S.; Jiang, Z. Friction and Wear Characteristics of TiO 2 Nano-Additive Water-Based Lubricant on Ferritic Stainless Steel. *Tribol. Int.* **2018**, *117*, 24−38.

(8) Ali, M. K. A.; Xianjun, H.; Mai, L.; Qingping, C.; Turkson, R. F.; Bicheng, C. Improving the Tribological Characteristics of Piston Ring Assembly in Automotive Engines Using Al2O3 and TiO2 Nanomaterials as Nano-Lubricant Additives. *Tribol. Int.* **2016**, *103*, 540−554.

(9) Binu, K. G.; Shenoy, B. S.; Rao, D. S.; Pai, R. A Variable Viscosity Approach for the Evaluation of Load Carrying Capacity of Oil Lubricated Journal Bearing with TiO 2 Nanoparticles as Lubricant Additives. *Procedia Mater. Sci.* **2014**, *6*, 1051−1067.

(10) Yin, X.; Wu, F.; Chen, X.; Xu, J.; Wu, P.; Li, J.; Zhang, C.; Luo, J. Graphene-Induced Reconstruction of the Sliding Interface Assisting the Improved Lubricity of Various Tribo-Couples. *Mater. Des.* **2020**, *191*, No. 108661.

(11) Restuccia, P.; Righi, M. C. Tribochemistry of Graphene on Iron and Its Possible Role in Lubrication of Steel. *Carbon* **2016**, *106*, 118−124.

(12) Guo, Y.-B.; Zhang, S.-W. The Tribological Properties of Multi-Layered Graphene as Additives of PAO2 Oil in Steel−Steel Contacts. *Lubricants* **2016**, *4*, No. 30.

(13) Eswaraiah, V.; Sankaranarayanan, V.; Ramaprabhu, S. Graphene-Based Engine Oil Nanofluids for Tribological Applications. *ACS Appl. Mater. Interfaces* **2011**, *3*, 4221−4227.

(14) La, D. D.; Truong, T. N.; Pham, T. Q.; Vo, H. T.; Tran, N. T.; Nguyen, T. A.; Nadda, A. K.; Nguyen, T. T.; Chang, S. W.; Chung, W. J.; Nguyen, D. D. Scalable Fabrication of Modified Graphene Nanoplatelets as an Effective Additive for Engine Lubricant Oil. *Nanomaterials* **2020**, *10*, No. 877.

(15) Zhao, W.; Ci, X. TiO 2 Nanoparticle/Fluorinated Reduced Graphene Oxide Nanosheet Composites for Lubrication and Wear Resistance. *ACS Appl. Nano Mater.* **2020**, *3*, 8732−8741.

(16) Du, S.; Sun, J.; Wu, P. Preparation, Characterization and Lubrication Performances of Graphene Oxide-TiO2 Nanofluid in Rolling Strips. *Carbon* **2018**, *140*, 338−351.

(17) Peng, Y.; Wang, Z.; Zou, K. Friction and Wear Properties of Different Types of Graphene Nanosheets as Effective Solid Lubricants. *Langmuir* **2015**, *31*, 7782−7791.

(18) Zhao, J.; Mao, J.; Li, Y.; He, Y.; Luo, J. Friction-Induced Nano-Structural Evolution of Graphene as a Lubrication Additive. *Appl. Surf. Sci.* **2018**, *434*, 21−27.

(19) Li, W.; Gao, L.; Liu, Y.; Ma, Z.; Wang, F.; Li, H. Preparation, Modification and Characterization of Plasma Sprayed Graphite/SiO2 Powder and Related Coating. *Ceram. Int.* **2019**, *45*, 2250−2257.

(20) Lang, C.; Ouyang, L.; Yang, L.; Dai, L.; Wu, D.; Shao, H.; Zhu, M. Enhanced Hydrogen Storage Kinetics in Mg@FLG Composite Synthesized by Plasma Assisted Milling. *Int. J. Hydrogen Energy* **2018**, *43*, 17346−17352.

(21) Dang, T. T.; Pham, V. H.; Hur, S. H.; Kim, E. J.; Kong, B.-S.; Chung, J. S. Superior Dispersion of Highly Reduced Graphene Oxide in N,N-Dimethylformamide. *J. Colloid Interface Sci.* **2012**, *376*, 91−96.

(22) Sahu, J.; Panda, K.; Gupta, B.; Kumar, N.; Manojkumar, P. A.; Kamruddin, M. Enhanced Tribo-Chemical Properties of Oxygen Functionalized Mechanically Exfoliated Hexagonal Boron Nitride Nanolubricant Additives. *Mater. Chem. Phys.* **2018**, *207*, 412−422.

(23) Singh, V. K.; Elomaa, O.; Johansson, L.-S.; Hannula, S.-P.; Koskinen, J. Lubricating Properties of Silica/Graphene Oxide Composite Powders. *Carbon* **2014**, *79*, 227−235.

(24) León, A.; Reuquen, P.; Garín, C.; Segura, R.; Vargas, P.; Zapata, P.; Orihuela, P. FTIR and Raman Characterization of TiO2 Nanoparticles Coated with Polyethylene Glycol as Carrier for 2-Methoxyestradiol. *Appl. Sci.* **2017**, *7*, No. 49.

(25) Singh, A.; Verma, N.; Mamatha, T. G.; Kumar, A.; Singh, S.; Kumar, K. Properties, Functions and Applications of Commonly Used

Lubricant Additives: A Review. *Mater. Today: Proc.* **2021**, *44*, 5018−5022.

(26) Krishnamurthy, A.; Abdul Razak, K.; Halemani, B. S.; Buradi, A.; Afzal, A.; Ahamed Saleel, C. Performance Enhancement in Tribological Properties of Lubricants by Dispersing TiO2 Nano-particles. *Mater. Today: Proc.* **2021**, *47*, 6180−6184.

(27) Jaiswal, V.; Kalyani; Umrao, S.; Rastogi, R. B.; Kumar, R.; Srivastava, A. Synthesis, Characterization, and Tribological Evaluation of TiO 2 -Reinforced Boron and Nitrogen Co-Doped Reduced Graphene Oxide Based Hybrid Nanomaterials as Efficient Antiwear Lubricant Additives. *ACS Appl. Mater. Interfaces* **2016**, *8*, 11698−11710.

(28) Lee, K.; Hwang, Y.; Cheong, S.; Choi, Y.; Kwon, L.; Lee, J.; Kim, S. H. Understanding the Role of Nanoparticles in Nano-Oil Lubrication. *Tribol. Lett.* **2009**, *35*, 127−131.

(29) Hamrock, B. J.; Dowson, D. Isothermal Elastohydrodynamic Lubrication of Point Contacts: Part III—Fully Flooded Results. *J. Lubr. Technol.* **1977**, *99*, 264−275.

(30) Huang, L.; Guo, D.; Shizhu, W. Film Thickness Decay and Replenishment in Point Contact Lubricated with Different Greases: A Study into Oil Bleeding and the Evolution of Lubricant Reservoir. *Tribol. Int.* **2016**, *93*, 620−627.

(31) Paul, G.; Hirani, H.; Kuila, T.; Murmu, N. C. Nanolubricants Dispersed with Graphene and Its Derivatives: An Assessment and Review of the Tribological Performance. *Nanoscale* **2019**, *11*, 3458−3483.

(32) Lee, C.; Li, Q.; Kalb, W.; Liu, X.-Z.; Berger, H.; Carpick, R. W.; Hone, J. Frictional Characteristics of Atomically Thin Sheets. *Science* **2010**, *328*, 76−80.

(33) Chouhan, A.; Mungse, H. P.; Sharma, O. P.; Singh, R. K.; Khatri, O. P. Chemically Functionalized Graphene for Lubricant Applications: Microscopic and Spectroscopic Studies of Contact Interfaces to Probe the Role of Graphene for Enhanced Tribo-Performance. *J. Colloid Interface Sci.* **2018**, *513*, 666−676.

(34) Soltanahmadi, S.; Morina, A.; van Eijk, M. C. P.; Nedelcu, I.; Neville, A. Investigation of the Effect of a Diamine-Based Friction Modifier on Micropitting and the Properties of Tribofilms in Rolling-Sliding Contacts. *J. Phys. D: Appl. Phys.* **2016**, *49*, No. 505302.

(35) Stankovich, S.; Dikin, D. A.; Piner, R. D.; Kohlhaas, K. A.; Kleinhammes, A.; Jia, Y.; Wu, Y.; Nguyen, S. T.; Ruoff, R. S. Synthesis of Graphene-Based Nanosheets via Chemical Reduction of Exfoliated Graphite Oxide. *Carbon* **2007**, *45*, 1558−1565.

(36) Nguyen-Phan, T.-D.; Luo, S.; Liu, Z.; Gamalski, A. D.; Tao, J.; Xu, W.; Stach, E. A.; Polyansky, D. E.; Senanayake, S. D.; Fujita, E.; Rodriguez, J. A. Striving Toward Noble-Metal-Free Photocatalytic Water Splitting: The Hydrogenated-Graphene−TiO 2 Prototype. *Chem. Mater.* **2015**, *27*, 6282−6296.

(37) Zhou, S.; Wu, Y.; Zhao, W.; Yu, J.; Jiang, F.; Wu, Y.; Ma, L. Designing Reduced Graphene Oxide/Zinc Rich Epoxy Composite Coatings for Improving the Anticorrosion Performance of Carbon Steel Substrate. *Mater. Des.* **2019**, *169*, No. 107694.

(38) Štengl, V.; Henych, J.; Vomáčka, P.; Slušná, M. Doping of TiO 2 -GO and TiO 2 -RGO with Noble Metals: Synthesis, Character-ization and Photocatalytic Performance for Azo Dye Discoloration. *Photochem. Photobiol.* **2013**, *89*, 1038−1046.

(39) Lin, C.; Yang, L.; Ouyang, L.; Liu, J.; Wang, H.; Zhu, M. A new method for few-layer graphene preparation via plasma-assisted ball milling. *J. Alloys Compd.* **2017**, *728*, 578−584.

(40) Wu, Y.; Yu, J.; Zhao, W.; Wang, C.; Wu, B.; Lu, G. Investigating the Anti-Corrosion Behaviors of the Waterborne Epoxy Composite Coatings with Barrier and Inhibition Roles on Mild Steel. *Prog. Org. Coat.* **2019**, *133*, 8−18.

(41) Voevodin, A. A.; Phelps, A. W.; Zabinski, J. S.; Donley, M. S. Friction induced phase transformation of pulsed laser deposited diamond-like carbon. *Diamond Relat. Mater.* **1996**, *5*, 1264−1269.

(42) Wang, D. S.; Chang, S. Y.; Huang, Y. C.; Wu, J. B.; Lai, H. J.; Leu, M. S. Nanoscopic observations of stress-induced formation of graphitic nanocrystallites at amorphous carbon surfaces. *Carbon* **2014**, *74*, 302−311.

(43) Ma, T.-B.; Hu, Y.; Wang, H. Molecular dynamics simulation of shear-induced graphitization of amorphous carbon films. *Carbon* **2009**, *47*, 1953−1957.

(44) Xu, Y.; Peng, Y.; Dearn, K. D.; Zheng, X.; Yao, L.; Hu, X. Synergistic Lubricating Behaviors of Graphene and MoS2 Dispersed in Esterified Bio-Oil for Steel/Steel Contact. *Wear* **2015**, *342−343*, 297−309.